

High Focusing-reflection Subwavelength Gratings with Uni-traveling-carrier Photodetector for High Responsivity

Qingtao Chen,^{1,3} Wenjing Fang,² Yongqing Huang,^{1,*} Xiaofeng Duan,¹ Kai Liu,¹ Mohammad S. Sharawi,³ and Xiaomin Ren¹

¹State Key Laboratory of Information Photonics and Optical Communications, Beijing University of Posts and Telecommunications, Beijing 100876, China

²Shandong Provincial Key Laboratory of Optical Communication Science and Technology, School of Physical Science and Information Technology, Liaocheng University, Liaocheng 252000, China

³Poly-Grames Research Center, Department of Electrical Engineering, École Polytechnique de Montréal, Montreal, QC H3T 1J4, Canada
*Corresponding author: yqhuang@bupt.edu.cn

Abstract: High focusing-reflection, non-periodic high-contrast grating integrated with a uni-traveling-carrier photodetector (FR-UTC-PD) is proposed to overcome the bandwidth-responsivity trade-off. The responsivity of the FR-UTC-PD is increased by 36.5% while achieving a 3-dB bandwidth of 18 GHz. © 2019 The Author(s)

OCIS codes: (050.6624) Gratings, (040.5160) Photodetectors.

1. Introduction

The single layer, high-index contrast subwavelength grating structures (i.e. high-contrast grating (HCG) with distinct constructed forms) can provide high focusing-reflection (FR), high transmission and high-quality-factor resonances. They have been extensively applied in the integration of different kinds of optoelectronic devices, such as vertical-cavity surface-emitting lasers (VCSELs), tunable VCSELs, sensors, resonators and hollow-core waveguides [1]. Moreover, periodic or non-periodic concentric-circular subwavelength gratings (serving as focusing reflectors) yielded great contributions to improve the responsivity of photodetectors (PDs) without sacrificing the high-speed response [2].

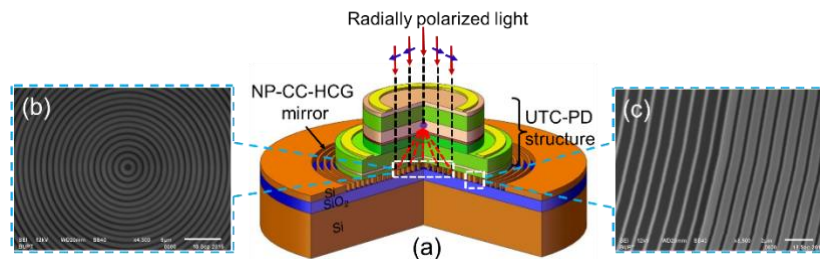


Fig. 1. (a) Schematic of an FR-UTC-PD consists a SOI-based NP-CC-HCG mirror integrated with a UTC-PD structure by wafer bonding. The scanning electron microscope (SEM) images locate (b) the center position, and (c) the non-periodic position of an NP-CC-HCG mirror.

The uni-traveling-carrier photodetector (UTC-PD) can achieve high-speed and high-saturation characteristics due to only adopting electrons as active carriers as well as the separating design of the absorption and collection layers [3-4]. Nevertheless, some constrains still exist among the above characteristics, especially how to exhibits a relatively high responsivity and a high bandwidth simultaneously. Therefore, it is particularly important to solve the bandwidth-responsivity trade-off in UTC-PDs. Moreover, some types of monolithically or quasi-monolithically integrated structures, such as resonant-cavity-enhanced UTC-PD (RCE-UTC-PD) [5] and high-reflectivity UTC-PD (HR-UTC-PD) [6], have been proposed to improve the responsivity of UTC-PDs. However, there still exists some problems in the process of time and cost for the epitaxial growth of distributed Bragg reflector (DBR) and complexities for the fabrication of monolithically integrated PD. In this paper, a high FR uni-traveling-carrier photodetector (FR-UTC-PD) structure, which experimentally realizes the integration of a high FR non-periodic concentric circular high-contrast grating (NP-CC-HCG) mirror with a high-speed UTC-PD by employing wafer-bonding technology, is reported to overcome the bandwidth-responsivity trade-off in UTC-PDs. The schematic design is shown in Fig.1 (a).

2. Focusing-reflection theory

The NP-CC-HCG mirror in an FR-UTC-PD consists of a set of concentric circular Si units with the thickness of 500 nm located on the top of a silicon-on-insulator (SOI) substrate, which is shown in Fig. 1 (a). The high-index Si grating

units surrounded by the adjacent air and a 500-nm-thick bottom SiO₂ layer with the low-indices of 1 and 1.46 constitute a high-index contrast grating structure, i.e. NP-CC-HCG mirror [7]. A focusing spot of the reflected light realized by NP-CC-HCG mirror can be obtained when the total phase shift meets the Eq. (1) [1]:

$$\phi(x) = \frac{2\pi}{\lambda} \left(f + \frac{\phi_{max}}{2\pi} \lambda - \sqrt{x^2 + f^2} \right) \quad (1)$$

where f is the focal length, λ is the wavelength, x is the radius of an NP-CC-HCG mirror, and ϕ_{max} is the maximum phase change.

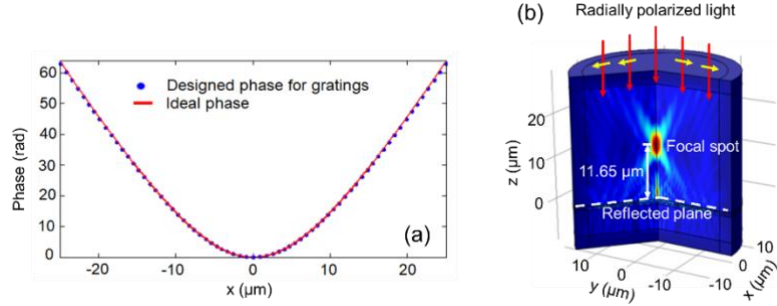


Fig. 2. (a) The calculated (the red line) and the simulated (the blue solid circles) phase distribution. (b) The FR ability simulation for the NP-CC-HCG mirror with a 12- μm setting focal length as an example.

For further analysis of the FR ability, the ideal phase distribution of the NP-CC-HCG mirror with a focal length of 12 μm is calculated by Eq. (1). The relevant simulation is implemented with a 1550-nm radially polarized light and the obtained results are shown in Fig. 2 (a). Obviously, the discrete non-periodic concentric circular grating bars along the x direction coinciding exactly with the theoretical calculation results. The FR ability of the NP-CC-HCG mirror is conducted by COMSOL implementing the finite element method (FEM) shown in Fig. 2 (b). The focus spot along the z -axis is 11.65 μm that is very close to the 12- μm theoretical setting value. Besides, the relevant field distribution full-width-half-maximum (FWHM) at the reflected focus plane is 0.8701 μm and a total FR efficiency of 92.1% is obtained at the reflected plane.

3. Results and discussion

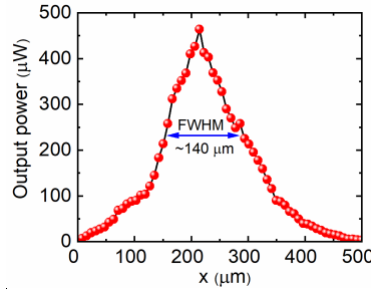


Fig. 3. Measured FR ability of an NP-CC-HCG mirror with a 1550-nm wavelength radially polarized light and a 3.56-mW input power.

The UTC-PD structure on top of the NP-CC-HCG mirror is mainly consisted of a 640-nm-thick p-type InGaAs absorption layer and a 500-nm-thick n-type InP collection layer. The formation of quasi-electric field in the absorption layer owing to the Gaussian-graded doping can help the electrons diffuse or drift rapidly to the collection layer. The undoped InGaAsP layer is applied to smooth the abrupt InGaAs/InP heterojunction. The double-mesa structure with p- and n-type Ohmic contacts are fabricated by conventional photolithography and wet etching technologies. Then the ground-signal-ground (GSG) coplanar waveguide Ti/Au-contact electrodes are landed on the surface of the polyimide passivation layer. After completing the fabrication of the UTC-PD, the InP substrate layer below n-type InP buffer layer is first grinded and then polished for the preparation of wafer bonding with the NP-CC-HCG mirror.

Meanwhile, the 500- μm -diameter NP-CC-HCG mirror with the focal length of 400 μm is fabricated by E-beam lithography (EBL) and inductively coupled plasma (ICP) dry etching. The SEM images in various locations are shown in Figs. 1 (b) and (c). Figure 3 is used to illustrate FR ability of the NP-CC-HCG mirror represented by the power distribution at the reflected focal plane. The measured results show that the reflected optical power approximately

presents Gaussian distribution along the x direction and the peak power locates at the middle position of the NP-CC-HCG mirror, which shows that this mirror has an excellent focusing ability. Moreover, the obtained maximum reflected optical power appears at the focal spot is $463.5 \mu\text{W}$ and the corresponding FWHM is $\sim 140 \mu\text{m}$, while an FR efficiency of 84.59% is achieved by integration. Subsequently, the FR-UTC-PD is realized by using wafer bonding to integrate the UTC-PD structure with the NP-CC-HCG mirror.

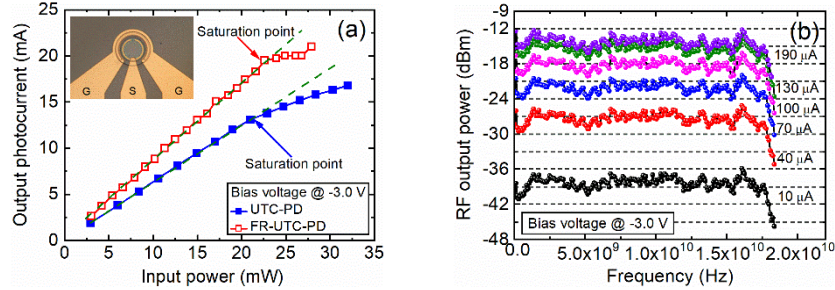


Fig. 4. (a) Measured output photocurrent versus input power (Inset: The top optical micrograph of a fabricated device), and (b) Frequency response for UTC-PD and FR-UTC-PD with $40\text{-}\mu\text{m}$ diameters at various output photocurrent levels.

Figure 4 (a) shows the measured DC saturation current for the UTC-PD and the FR-UTC-PD under the bias voltage of -3.0 V and a 1550-nm wavelength excitation. The linear parts show that the output photocurrent gradually increases with the increase of the input power until up to a saturation point, which reveals the responsivity characteristic of the device. The relevant responsivity is 0.63 A/W and 0.86 A/W for UTC-PD and FR-UTC-PD, respectively. Compared to the UTC-PD without the NP-CC-HCG mirror, it is obvious that the responsivity of FR-UTC-PD is increased by 36.5%. This is because the NP-CC-HCG mirror makes the FR-UTC-PD get almost twice the effective absorption efficiency from the incident light than that of the UTC-PD. Moreover, the responsivity of the FR-UTC-PD could be improved by reasonably designing the focal length of the NP-CC-HCG mirror to make more reflected light to be absorbed by the absorption layer. Fig. 4 (b) shows the measured frequency response of FR-UTC-PD and UTC-PD in a series of low output photocurrent levels. It can be seen the 3-dB bandwidth of all is 18 GHz at a bias voltage of -3.0 V and a 1550-nm wavelength source. Therefore, there is no effect on the bandwidth of the UTC-PD with or without an NP-CC-HCG mirror.

4. Conclusions

A high-performance FR-UTC-PD resulting from integrating an NP-CC-HCG mirror and a UTC-PD structure is reported to overcome the trade-off between responsivity and bandwidth in UTC-PDs. The FR ability of an NP-CC-HCG mirror is analyzed theoretically with the obtained focal length of $11.65 \mu\text{m}$. The field distribution FWHM at the reflected focal plane is $0.8701 \mu\text{m}$ and the FR at the reflected plane is 92.1%. For a fabricated NP-CC-HCG mirror with $400 \mu\text{m}$ focal length, the reflected optical power is $463.5 \mu\text{W}$, the corresponding FWHM is $\sim 140 \mu\text{m}$ and the calculated FR efficiency is 84.59%, all are achieved using a 1550-nm wavelength radially polarized light. The FR-UTC-PD is realized by using wafer bonding technology and the obtained responsivity is 0.86 A/W showing an improvement of 36.5% in comparison with a UTC-PD without an NP-CC-HCG mirror. The 3-dB bandwidth of the FR-UTC-PD is neither increased nor degraded compared with that of the UTC-PD without an NP-CC-HCG mirror.

5. Acknowledgements

This work is supported by the National Natural Science Foundation of China (NSFC) under the Grant Nos. 61574019, 61674018 and 61674020. The authors thank Jiarui Fei and Tao Liu for the assistance with measurements.

6. References

- [1] C. J. Chang-Hasnain and W. Yang, "High-contrast gratings for integrated optoelectronics," *Adv. Opt. Photonics* 4, 379-440 (2012).
- [2] X. Duan *et al.*, "High efficiency InGaAs/InP photodetector incorporating SOI-based concentric circular subwavelength gratings," *IEEE Photon. Technol. Lett.*, vol. 24, no. 10, 863-865 (2012).
- [3] T. Ishibashi *et al.*, "Uni-traveling-carrier photodiodes," in *Ultrafast Electron. Optoelectron. Tech. Dig.*, 83-87 (1997).
- [4] H. Ito *et al.*, "InP/InGaAs uni-traveling-carrier photodiode with 310 GHz bandwidth," *Electron. Lett.*, vol. 36, no. 21, 1809-1810 (2000).
- [5] D. Miao *et al.*, "Structure optimization of resonant cavity-enhanced uni-travelling carrier photodiode for high quantum efficiency and wide optical bandwidth," in *Proc. Asia Commun. Photon. Conf. (Opt. Soc. Amer.)*, paper ATH3A.51 (2014).
- [6] Q. Chen *et al.*, "Uni-traveling-carrier photodetector with high-reflectivity DBR mirrors," *IEEE Photon. Technol. Lett.*, vol. 29, no. 14, 1203-1206 (2017).
- [7] W. Fang *et al.*, "Concentric circular focusing reflector realized using high index contrast gratings," *Opt. Commun.*, vol. 402, 572-576 (2017).